Chapter 12
Membrane Excitation and Cytoplasmic Streaming as Modulators of Photosynthesis and Proton Flows in Characean Cells

A. A. Bulychev

Abstract Internodal cells of *Chara corallina* represent a unique model system to study interactions between photosynthesis, membrane excitation, and cytoplasmic streaming, as well as the role of these processes in generation and regulation of functional patterns in green cells and tissues. It is established that the inflow of cytoplasm from darkened cell parts promotes photosynthetic activity of chloroplasts residing at intermediate irradiance, whereas the arrival of cytoplasm from illuminated regions suppresses this activity and enhances nonphotochemical quenching. The vectorial movement of the "irradiated" cytoplasm induces functional asymmetry around the light spot (pattern formation) both in the chloroplast layer and in the plasma membrane. The messenger transported between illuminated and shaded cell parts was found to move at the velocity of cytoplasmic streaming. The effects of membrane excitation (action potential) on photosynthesis and membrane H^+ transport are area specific; they are mediated by different mechanisms under physiological conditions and in the presence of some redox-cycling compounds. The influence of action potential on chlorophyll fluorescence under spot illumination appears to involve the activation of Ca^{2+}-mediated pathways and the suppression of metabolite exchange between darkened and illuminated cell parts due to the stoppage of cyclosis. The cytoplasmic flow from darkened to illuminated cell parts seems to enhance interactions between respiratory and light-dependent metabolism, which promotes photosynthesis and protects chloroplasts from photooxidative damage under excess light.

A. A. Bulychev (✉)
Department of Biophysics, Biology, Moscow State University,
Moscow 119991, Russia
e-mail: bulychev@biophys.msu.ru

Abbreviations

AOI	area of inspection where external pH and chlorophyll fluorescence are measured in *Chara* internodal cell;
AP	action potential;
CB	cytochalasin B;
DTT	dithiothreitol;
MV	methyl viologen;
NPQ	nonphotochemical quenching;
pH_c	cytosolic pH;
pH_o	pH near the cell surface in the outer medium;
PM	plasma membrane;
PFD	photon flux density;
PSI and PSII	photosystems I and II;
ROS	reactive oxygen species;
$\Delta F/F_m'$	effective quantum yield of electron transport in PSII

12.1 Introduction

The cells and tissues of green plants can undergo reversible transitions between spatially uniform and patterned distribution of photosynthetic activity upon illumination and darkening. When the dark-adapted leaf is exposed to light, the initial homogeneous images of chlorophyll fluorescence are replaced with the mosaic of patches showing damped oscillations (Siebke and Weis 1995; Schurr et al. 2006; Baker 2008). The origin of pattern emergence in the seemingly uniform system is still far from being clarified. The spatial distribution of photosynthetic activity is tightly related to the formation of nonuniform electrochemical proton gradients across the thylakoid and plasma membranes (PMs) (Bulychev and Vredenberg 2003; Krupenina and Bulychev 2007). Although plant cells possess various photoreceptors (phytochrome, phototropins, etc.), the light responses of membrane transport in green cells are usually mediated by chloroplasts (Marten et al. 2010). Illuminated leaves of aquatic plants acidify the medium adjacent to the lower leaf side, but elevate pH at the opposite leaf side (Prins et al. 1982). This polarity of H^+ transport, beneficial for CO_2 acquisition, indicates that electron- and ion-transport reactions in chloroplasts may activate divergent regulatory pathways resulting in either H^+ influx or efflux at the cell level.

Single cell systems, such as Characean internodes, provide a unique biological model for studying the photosynthetic and H^+ transport patterns. In dark-adapted internodal cells, the potential photosynthetic activity and properties of the PM are spatially uniform. However, the cells exposed to light produce alternating acidic and alkaline bands or asymmetric patches on the outer cell surface. Although the

occurrence of pH bands in Characeae and their possible influence on photosynthesis has been known for almost 40 years (Spear et al. 1969; Lucas 1975a), the first clear-cut evidence for close correlation between the pH banding and photosynthetic activity of chloroplasts in the underlying cell regions was presented much later (Bulychev et al. 2001a). The cell areas producing acid and alkaline pH zones feature high and low photosynthetic rates, respectively (Bulychev et al. 2005), which is clearly evident from imaging of chlorophyll fluorescence and pH bands (Krupenina et al. 2008).

The concerted emergence of pH and photosynthetic bands awaits deeper interpretation. A compelling task is to reveal key factors involved in formation and regulation of these labile patterns. Recent findings emphasized significance of intracellular transport and signaling events. Specifically, the cytoplasmic streaming and electrical excitation of the PM were found engaged in generation and triggered elimination of the pH bands as well as in modulation of chloroplast activity.

Cytoplasmic streaming (cyclosis) enables lateral distribution of substances and vesicles over long distances, at which diffusion is ineffective (Kamiya 1959; Verchot-Lubicz and Goldstein 2010). This function is particularly important for giant cells, such as internodes of Characean algae. The flow of liquid along immobile chloroplasts greatly accelerates the exchange of solutes between organelles and fluids (Pickard 2003; Goldstein et al. 2008). The velocity of cytoplasmic streaming in Characean internodes (up to 100 μm/s) is at the highest limit detected for plant cells. The cytoplasm movement in *Chara* cells is determined by interaction of subcortical actin bundles attached to the inner side of immobile chloroplasts and myosin molecules bound to freely moving organelles in the endoplasm (Shimmen and Yokota 2004). Despite general recognition of vital significance of cyclosis, there is surprisingly scarce data concerning its role in specific cell functions.

Propagation of electric signals in plants has been a matter of numerous studies (Davies 2006; Fromm and Lautner 2007; Krol et al. 2010). Electric signals basically similar to action potentials (AP) of animal cells are obvious in sensitive and carnivorous plants, like *Mimosa* and *Dionaea*, and are also propagated in plants lacking visible movement reactions. The long-distance transmission of electric signals along the conducting bundles after flame injury or mechanical stimulation was found to suppress photosynthesis in leaves (Koziolek et al. 2003; Grams et al. 2009; Pavlovic et al. 2011). The assignment of photosynthesis inhibition to propagation of AP is somewhat obscured by the transmission of both electric and hydraulic signals in response to flame stimuli (Stahlberg and Cosgrove 1997; Fromm 2006). Furthermore, two types of electrical signals can propagate along the conducting tissues after heat injury: AP and variation potentials. Unlike AP, variation potentials are characterized by variable depolarization amplitude, longer duration, and a slower spreading velocity. The inhibitory influence of variation potentials on photosynthesis has long been noted (Van Sambeek and Pickard 1976).

Ambiguity related to different nature of transmitted signals can be avoided by monitoring the photosynthetic activity of individual excitable cells, such as giant

internodes of Characean algae that are capable of generating AP in a controlled and reproducible manner on passing a short pulse of transmembrane electric current. Characean algae are perfectly suitable for studying interrelations between membrane excitability, cytoplasmic streaming, photosynthesis, and pattern formation, because they exhibit all these basic phenomena at the cell level. The essential advantage is that Characean chloroplasts are immobile and produce a densely packed single layer array.

This review outlines current knowledge on relations between the transmembrane H^+ flows and photosynthetic activity and highlights the role of cyclosis and electrical membrane excitation in creation and regulation of external pH pattern and chloroplast functions. Related topics are dealt with in the present volume (Beilby) and were surveyed previously (Bulychev and Krupenina 2008c, 2010).

12.2 Light-Dependent Patterns in Resting *Chara corallina* Cells

12.2.1 Significance of pH Banding

One may wonder why it is important to analyze alkaline zone formation and whether the segregation of alkaline and acid regions is a specific trait of Characean algae, having little relevance to other plant species. Apart from the key role of membrane H^+ transport in regulation of cytoplasmic pH, electrogenesis, and mineral nutrition (Palmgren 1998; Tazawa 2003), several further points should be noted.

1. Spatial separation of H^+-extruding and H^+-absorbing zones is not unique to charophytes and is observed in other systems, e.g., growing pollen tubes (Feijo et al. 1999), root tips (Felle 1998), fungal hyphae (Gow et al. 1984), and leaves of aquatic plants (Prins et al. 1982). The polarity of H^+ fluxes across the PM on different leaf sides is benefit to photosynthesis of aquatic plants inhabiting weakly alkaline stagnant waters, since local acidification shifts the HCO_3^-/CO_2 equilibrium ($pK_1 \sim 6.35$) to higher concentration of permeant neutral species (CO_2) and provides available substrate for photosynthesis (Walker et al. 1980; Prins et al. 1982; Plieth et al. 1994).

2. The elevation of external pH by photosynthesizing cells underlies biogenic calcification (Borowitzka 1987; McConnaughey 1991; Jansson and Northen 2010). At alkaline pH the HCO_3^-/CO_3^{2-} equilibrium ($pK_2 \sim 10.3$) is shifted toward the formation of CO_3^{2-}, which precipitates $CaCO_3$ and depletes Ca^{2+} in the alkaline zones. The resulting variations of Ca^{2+} in the apoplast might be involved in regulation and differentiation of plant growth and development. Mineralization at high pH is documented for cyanobacteria, green algae, e.g., *Halimeda*, and marine plankton algae; it is also important for coral growth.

3. According to the "acid growth theory," the acidic pH of the apoplast weakens cross-linking bonds in cell walls and loosens the cell wall matrix, thus favoring

the plant cell elongation (Rayle and Cleland 1992; Palmgren 1998; Hager 2003). Multiple sites of cell elongation in Characean internodes are restricted to the areas of external acidity (Metraux et al. 1980).

4. The breaking up of uniform pH distribution along the outer cell surface is an early step in formation of cell polarity. The emergence of asymmetry, fixed in ionic and molecular gradients, is a crucial stage in light-dependent morphogenesis, e.g., in developing *Fucus* zygotes (Coelho et al. 2008).

5. The striking heterogeneity of membrane properties in Characean cells was not taken into consideration in many, otherwise excellent, studies concerning light-dependent ion transport, operation of the electrogenic H^+ pump and ion channels in this model system (Tazawa 2003). Clearly, the assumption of homogeneous distribution of ion transport systems over the cell surface is inapplicable in many cases.

12.2.2 Pattern Visualization

The light-dependent pH patterns are readily visualized with indicator dyes phenol red (Spear et al. 1969; Shimmen and Wakabayashi 2008) and thymol blue (Beilby et al. 1993; Eremin et al. 2007). Phenol red is convenient for qualitative detection of alkaline bands. It is unsuitable for evaluation of pH shifts, since its color response is saturated at $pH \geq 8$, while actual values in the alkaline zones approach pH 10. Therefore, pH changes as large as two pH units can be simply overlooked.

The antimony-based pH microelectrodes, featuring the linear function of pH and high temporal resolution (~ 1 s), are perfect for quantitative pH measurements in the regime of scanning along the cell at the velocity of ~ 10 mm/min (Bulychev et al. 2001b). They are also appropriate for tracking the kinetics of surface pH (pH_o).

Vibrating electrodes proved suitable for mapping the extent and direction of extracellular currents. The routes of electric current correspond to longitudinal pH profiles, with outward current extending from acid zones and the inward current being confined to alkaline zones (Lucas and Nuccitelli 1980). A minor drawback is interference from stirring of external medium by periodic movement of the probe.

Heterogeneous profiles of the membrane potential and the PM conductance were measured with the "water-film electrode" (Ogata et al. 1987). Based on this method, the low-conductance cell regions with the hyperpolarized membrane potential were detected and ascribed to acidic zones. By contrast, the alkaline regions were identified as high-conductance depolarized regions.

Photosynthetic activity in vivo on a microscopic level can be assessed from measurements of chlorophyll fluorescence with the saturation pulse technique [reviewed in (Schreiber 2004)]. The method provides information on the effective quantum yield of electron transport in photosystem II (PSII) ($\Delta F/F_m'$) and on nonphotochemical fluorescence quenching (NPQ), a parameter derived from the Stern–Volmer equation and describing the protective heat dissipation of excess

energy. The actual rate of linear electron flow is proportional to the product of $\Delta F/F_m'$ and the photon flux density (PFD). The longitudinal profiles were measured with point-by-point resolution using Microscopy PAM (pulse-amplitude-modulation) fluorometer (Walz, Germany) and by means of chlorophyll fluorescence imaging (Imaging-PAM Chlorophyll fluorometer, Walz) (Krupenina et al. 2008).

Chlorophyll fluorescence of PSII under weak actinic light is low, since most excitations are spent for charge separations. The saturation light pulse reduces the primary acceptor Q_a, which inhibits the photochemical activity of PSII and enhances fluorescence and energy losses to heat. The effective quantum yield $\Delta F/F_m'$ is calculated from fluorescence measured before and during the saturation pulse (F and F_m', respectively): $\Delta F/F_m' = (F_m' - F)/F_m'$. The parameter NPQ is evaluated from the equation: $NPQ = (F_m - F_m')/F_m'$, where F_m and F_m' designate maximal fluorescence induced by the saturation pulse in the dark-adapted sample and in the same sample exposed to actinic light ($F_m' < F_m$).

The lower values of F_m' compared to F_m reflect the increased thermal losses that are related directly and indirectly to acidification of the thylakoid lumen and ΔpH formation (Finazzi et al. 2004). Thus, NPQ can be used as an indicator of the thylakoid ΔpH. In support of this notion, nonphotochemical quenching in *Chara* cells vanished in the presence of the ionophores nigericin and monensin known to eliminate the thylakoid ΔpH (Bulychev and Kamzolkina 2006). Simultaneous profiling of NPQ and pH_o along *C. corallina* cells revealed their parallel changes, indicating that the thylakoid ΔpH is high in the alkaline cell regions and low in areas with acidic external pH (Krupenina and Bulychev 2007).

Net photosynthetic activity was also assessed amperometrically with glass-insulated platinum electrode whose current is sensitive to O_2 content near the cell surface. When longitudinal profiles of external pH and O_2 concentration were compared, the positions of alkaline peaks coincided with minima of O_2 content, while the acidic regions corresponded to the peaks of O_2 level (Bulychev et al. 2001a). The antiparallel profiles of pH and pO_2, combined with fluorescence data, confirmed the faster rates of PSII electron flow in the acidic cell regions. They might also indicate the electron transport to O_2 in alkaline cell regions.

Cytological studies revealed that cortical mitochondria are relocated under light to photosynthetically active acid regions (Foissner 2004; Braun et al. 2007). Staining *Chara* cells with fluorescent markers of acidic organelles (the PM invaginations charosomes) and with markers of H^+-ATPase revealed their colocalization in the cell regions producing acidic bands (Schmölzer et al. 2011). This confirms the association of the PM H^+-pump with the membrane domains producing acid zones.

Thus, multiple manifestations of spatial heterogeneity in illuminated Characean cells include pH bands or patches, variations in chlorophyll fluorescence and photosynthetic activity, different extents of NPQ and the thylakoid ΔpH, differential conductance and membrane potentials, bands or patches of calcium precipitations, nonuniform distribution of mitochondria, area-specific growth rates, stronger adhesion of water to the cell surface in alkaline regions (Dorn and Weisenseel 1984), and enrichment of acidic cell regions with H^+-ATPase activity.

12.2.3 Coordination of Photosynthetic and pH Patterns

It is generally agreed that photosynthesis is a prerequisite for the band formation; no banding occurs in the presence of diuron, an inhibitor of photosynthetic electron flow. Photosynthesizing chloroplasts act as a source or a sink of some metabolites (e.g., H^+, ATP, Ca^{2+}, or phosphate) during the exchange of these species across the plastid envelope. At low irradiance the cell may exhibit a single band, while the number of bands increases with light intensity (Lucas 1975a; Bulychev et al. 2003).

One hypothesis for coordination of photosynthetic and pH bands is that chloroplasts of acid and alkaline cell regions differ in ATP-synthesizing capacity (Bulychev et al. 2005; Bulychev and Krupenina 2008c). In those regions where the thylakoid ΔpH is not readily utilized for ATP synthesis, higher amounts of protons accumulate in the thylakoid lumen, thus restricting the photosynthetic electron flow (photosynthetic control). The extensive H^+ uptake by thylakoids is supposed to deplete protons in the chloroplast stroma and the cytoplasm (Hansen et al. 1993). The ATP deficiency and high cytoplasmic pH preclude the operation of PM H^+ pump (Hager 2003), which elevates pH on the outer surface (pH_o) and activates the high pH channels whose conductance increases dramatically with the external pH (Bisson and Walker 1980). These channels account for the unusually high area-specific membrane conductance in the alkaline cell regions of illuminated cells (Walker et al. 1980). The downhill H^+ influx through the opened high pH channels will further elevate pH_o, diminish CO_2 content, and suppress the assimilating electron flow.

Conversely, in the regions where chloroplasts rapidly produce ATP for CO_2 fixation, the thylakoid ΔpH is consumed for ATP synthesis and remains low (Finazzi et al. 2004). The cytoplasmic ATP content is not depleted, thus promoting the H^+ pump operation, which creates the acidic external pH. The local acidification near the cell surface converts the membrane-impermeable anion HCO_3^- to the neutral readily permeant species, CO_2. This provides the cell with a carbon substrate and ensures high photosynthetic rates. The sufficiency of ATP for operation of PM H^+-pump in the acidic cell regions is further promoted by gathering of cortical mitochondria in the regions with high photosynthetic activity.

In the above scheme, the PM H^+-ATPase is considered as a generator of outward current, while the inward current in alkaline regions is carried either by H^+ influx or OH^- efflux. Because of the feedback relations, the system homogeneous in darkness can become unstable at light conditions and produce bands with spatially distributed H^+ pumps and H^+ leaks.

Segregated cell areas accommodate hundreds of thousands chloroplasts, which may cast some doubt on the assumption that photosynthetic and pH bands arise from microscopic fluctuations in a spatially uniform distribution. It should be noted, however, that pH zones appear at early stages as numerous minute pH excursions (Bulychev et al. 2001b). These fluctuations transform later to long-lived patches and finally rearrange to radially symmetric bands (Bulychev et al. 2003). Hence, emergence of bands from fluctuations in the originally homogeneous system cannot be excluded.

On the other hand, uniform illumination of the chloroplast layer is hardly ever achieved. Each internode of *C. corallina* contains two helical chloroplast-free narrow lines (equal in width to few chloroplast rows) that separate counter-directed cytoplasmic flows [see, e.g., diagrams in (Verchot-Lubicz and Goldstein 2010)]. At places where these neutral zones intersect the pathway of incident light, they act as transparent windows in the dense chloroplast layer and transmit narrow light beams to the underlying cell side.

If positions of alkaline bands depend on the intracellular pattern of light spots imposed by spiraling chloroplast-free lines and the bands are not structurally fixed (e.g., by calcification or charosomes), the band pattern should be sensitive to angular direction of incident light. Although this possibility remains untested, the role of nonuniform illumination in generation of photosynthetic and pH bands was verified with the use of localized lighting. A narrow beam applied through a thin light guide, can mimic the light spot projected by the chloroplast-free indifferent zone.

12.3 Role of Cyclosis in pH Pattern Formation

The chloroplast–PM interactions outlined above are mediated by the cytoplasm that acts as an intermediary pool of substances transported across PM and the chloroplast envelope upon the onset of photosynthesis and upon activation or inactivation of ion pumps and channels. However, the suggested scheme is static in a sense that rapid cytoplasmic flow is omitted from consideration.

Some mathematical models based on the reaction–diffusion system simulated the appearance of pH bands in *Chara* without implicating the cytoplasmic flow. It was assumed that active and passive H^+ flows across PM depend on the driving force for protons as well as on voltage-controlled operation of the PM H^+-pump and passive H^+ leak (Plyusnina et al. 2005). Other theoretical models comprised cyclosis as an essential element of pattern formation in *Chara* (Bulychev et al. 2001b).

Despite generally recognized role of cyclosis in vital cell functions, little is known about the influence of cytoplasmic streaming on membrane transport and photosynthesis. According to early studies (Lucas and Dainty 1977), the inhibition of streaming with cytochalasin B (CB) had no effect on the rate of photosynthetic CO_2 fixation in *C. corallina* cells exposed to overall illumination. Nevertheless, this conclusion, valid for uniform lighting conditions, may be inapplicable to a more general case of inhomogeneous illumination.

12.3.1 Polarity of pH Patch Formation Around the Light Spot

Application of a narrow light beam, combined with local measurements of pH_o and chlorophyll fluorescence provided new insights into the role of cyclosis in pattern formation (Bulychev and Dodonova 2011; Dodonova and Bulychev 2011).

If chloroplasts in illuminated region release or deplete some functional metabolite, the altered cytoplasm would flow downstream of the illuminated area and may affect the operation of chloroplast and plasmalemma systems in shaded areas. Conversely, in regions located upstream of the lightened area, the cytoplasm composition would be the same as in darkened cell parts. Hence, the cell regions exposed to identical light conditions at equal distances from the light spot might differ in their properties, thus mimicking the pattern formation.

This assumption was verified by measuring the surface pH (pH_o) and chloroplast fluorescence at equal distances on opposite sides from the light spot. For pH_o measurements, the area of inspection (AOI) was selected after checking its ability to generate alkaline zones. The localized beam was applied sequentially upstream and downstream of AOI with regard to the direction of cytoplasmic flow. Light emitted by a diode source (neutral white light, Luxeon, Lumileds, USA) was directed to the cell through a flexible light guide with a core diameter of 2.0 or 0.4 mm. The position of the fiber optics with respect to AOI was adjusted with micrometric screws. The alkaline zone in AOI was first preformed under overall illumination, and then it was allowed to dissipate gradually in darkness. After pH_o dropped to a certain level, the localized illumination was switched on. The subsequent pH changes in AOI differed greatly depending on the position of the light spot upstream or downstream of AOI, while the examined area stayed in the shade at equal distances d from the fiber optic core.

When the 2 mm-wide light guide was positioned 1–5 mm downstream of AOI, the onset of local illumination had no effect: the pH_o continued to decrease smoothly toward the bulk pH, with the same kinetics as in darkness (Fig. 12.1). By contrast, when the light guide was placed upstream of AOI at the same distance, a steep formation of alkaline zone was observed. An evident explanation for asymmetric formation of pH patch around the light spot is that illuminated chloroplasts alter the composition of flowing cytoplasm by virtue of ion or metabolite exchange across the envelope membrane, while the flow of modified cytoplasm affects the operation of H^+ (OH^-) transport in the shaded downstream regions. Other possible causes were considered and discarded. In particular, the profiles of residual irradiance against the distance from the light–shade border were identical regardless of the light spot position upstream or downstream of AOI (Dodonova and Bulychev 2011).

12.3.2 Necessity of Dim Light in the Area of Patch Formation

The narrow light beam directed straight to AOI produced no alkaline zone in this area (Bulychev et al. 2001b; Bulychev and Vredenberg 2003). The alkaline patch emerged downstream of the light spot at a short distance from the light–shade border, at a location where irradiance was not zero because of the scattered and reflected stray light. Dim background irradiance at AOI seems essential for generation of the alkaline zone. This notion relies on a series of experiments in which the light beam was directed upstream of AOI through a narrow (0.4 mm) optic

Fig. 12.1 Asymmetric changes of surface pH (pH_o) in response to local illumination applied 2 and 2.5 mm upstream (*curves 1* and *2*, respectively) and 2 mm downstream (*curve 3*) of AOI in *C. corallina* cell. *Arrow* marks the onset of localized illumination (white light, 1,500 µmol m^{-2} s^{-1}, beam width 2 mm). The indicated distances designate the space between AOI and the edge of the light guide core
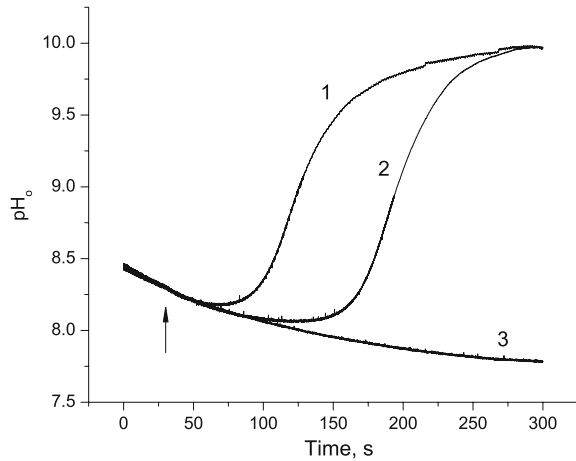
fiber under the angle of 30° to the horizontal plane to reduce stray light. The irradiance around the light spot was controlled by the background overall illumination that was switched on 60 s prior to localized lighting.

When a narrow beam of intense light (500 µmol m^{-2} s^{-1}) was applied upstream of AOI in addition to dim background light (9 µmol m^{-2} s^{-1}), the alkaline patch was formed in a marked similarity to curve 1 in Fig. 12.1. In the absence of dim background light the application of localized beam did not produce the alkaline patch, and the pH_o declined as in Fig. 12.1, curve 3. The presence of background light without the localized beam was also ineffective.

Apparently, two conditions should be fulfilled for the induction of alkaline patch: (1) AOI should be flushed by "irradiated" cytoplasm and (2) weak background irradiance at AOI is needed. Both conditions are apparently satisfied during unilateral illumination of the whole cell. The transparent spiraling zones create the periodic light pattern at the bottom chloroplast layer, and cyclosis ensures the delivery of cytoplasm across the light–shade interface. The necessity of dim light in AOI indicates that the patch formation involves not only chloroplasts of brightly lit "source area" but also the plastids of shaded "sink" zone. At variance with this notion, the alkaline zone was observed in chloroplast-free cell parts that were obtained by wounding (Shimmen and Yamamoto 2002). Apparently, the mechanisms of alkaline zone formation may differ slightly for intact and wounded cells.

12.3.3 Photosynthesis Versus Photodamage as a Primary Cause of Alkaline Patch Formation

Intensities of local illumination indicated above were severalfold higher than the reported value of 15–20 W/m^2 for saturation of photosynthesis in *C. corallina* (Lucas 1975b). In order to prove that the effects of local illumination were not

caused by injuring action of strong light, the intensity of narrow beam directed through a 2 mm wide fiber optics was lowered to various extents. When PFD was reduced in the range from 1,500 to 190 μmol m^{-2} s^{-1} (in the absence of background overall illumination), alkaline patches with equally high pH_o were formed after the lag periods increasing from 30 to 75 s (Dodonova and Bulychev 2011). The longer lag periods at reduced PFD were probably related to lower intensities of stray light in AOI in the absence of supplemental background illumination. It was concluded that the alkaline zone is formed at a wide range of light intensities and that the high light stress is not essential in this process.

Considering the actual photon flux created by narrow beam in AOI on the lower cell side, it should be noted that the upper chloroplast layer attenuates the transmitted light nearly 3-fold (the absorbance of *C. corallina* internode ~ 1.0 in the peak of chlorophyll absorption is divided between the upper and lower chloroplast layers). When the light guide was inclined at an angle of $30°$ to the horizontal plane, the irradiance at the cell bottom diminished additionally at least 2-fold (sin $30° = 0.5$). It means that, at PFD of 500 μmol m^{-2} s^{-1}, the chloroplasts in AOI were exposed to 6-fold lower photon flux.

Such flux densities can be considered physiologically relevant, because Characean algae in natural environments may endure PFD up to few hundred micromoles per 1 m^2 per second. The solar radiation on a cloudless summer day is about 2,300 μmol m^{-2} s^{-1} [e.g., (Takakura and Fang 2002)]. In typical freshwater lakes, light is attenuated with depth to 1% at a level of 10 m below the surface (Nobel 2005). Characean algae (e.g., *Nitellopsis*) grow well at about 3 m below the surface, where PFD should be attenuated approximately 4-fold compared to the surface value. The algal cells can apparently cope with negative effects of short exposures to such irradiance.

12.3.4 Effects of Cyclosis Cessation

After the generation of AP, cyclosis stops immediately for about 30 s and fully recovers within about 5 min. When the AP was triggered few seconds before the onset of the local light applied upstream of AOI, the formation of alkaline patch was strongly delayed and pH_o increased insignificantly during the observation period (Dodonova and Bulychev 2011). This finding is consistent with the assumed lateral transfer of a mediator but is not entirely conclusive, because the influence of AP on pH bands may be also caused by the increase in cytosolic Ca^{2+} content and consequent Ca^{2+}-triggered events.

Cytochalasin B is a specific inhibitor of cytoplasmic streaming (Bradley 1973; Foissner and Wasteneys 2007). During incubation in the presence of CB the streaming decelerates and eventually ceases. The alkaline patch formation caused by localized lighting (as shown in Fig. 12.1) was consistently delayed during cyclosis retardation. This delay was quantified by fitting the pH_o changes with the sigmoid curves. Both cyclosis and the light-induced formation of alkaline zone

were restored during the cell wash after the removal of CB from the medium
(Dodonova and Bulychev 2011). The streaming velocity and the half-time $t_{1/2}$ of
alkaline patch formation changed in opposite directions during and after the CB
treatment. The inverse of the time $t_{1/2}$ was taken as a measure of the rate constant
of alkaline zone formation. The plot of this rate constant against the streaming
velocity was linear, with the slope of straight line ~ 1 cm^{-1}.

12.4 Influence of Cyclosis on Chlorophyll Fluorescence and Photosynthesis

Considering tight relations between photosynthetic and pH patterns, a question
arises of how the chloroplasts residing at intermediate irradiance respond to the
delivery of cytoplasm from brightly illuminated and shaded areas. This issue was
studied by means of localized lighting applied through a thin (0.4 mm) optic fiber
inclined at 30° to horizontal plane. Weak background light was permanently
imposed on the whole cell to provide controlled PFD on the shaded part of the
interface (Bulychev and Dodonova 2011).

12.4.1 Cyclosis-Mediated Polarity of Distant Interactions Between Chloroplasts

Figure 12.2 shows changes of F_m' fluorescence in AOI that were induced by
localized light (500 μmol m^{-2} s^{-1}) applied through a thin optic fiber in addition to
permanent whole cell illumination of intermediate intensity (28 μmol m^{-2} s^{-1}).
Curves 1 and 2 represent F_m' changes in AOI when the optic fiber was positioned
1 mm upstream and downstream of AOI, respectively, with regard to the direction
of cytoplasmic flow. In the case of delivery of "irradiated" cytoplasm to AOI from
the illuminated upstream area, the narrow beam induced strong quenching of F_m'
after a distinct lag period. When the optic fiber was shifted downstream of AOI,
F_m' remained unaffected.

The origin of this asymmetry for distant interactions between illuminated and
shaded chloroplasts is similar to that of pH patch formation around the light spot.
Apparently, the chloroplasts of brightly illuminated area release or absorb some
ion or substance that acts like a messenger and moves vectorially with the cyto-
plasmic flow along the cell. When the modified cytoplasm arrives to remote
chloroplasts in AOI residing at moderate irradiance, F_m' is quenched (curve 1).
The background irradiance did not quench F_m' when the modified cytoplasm
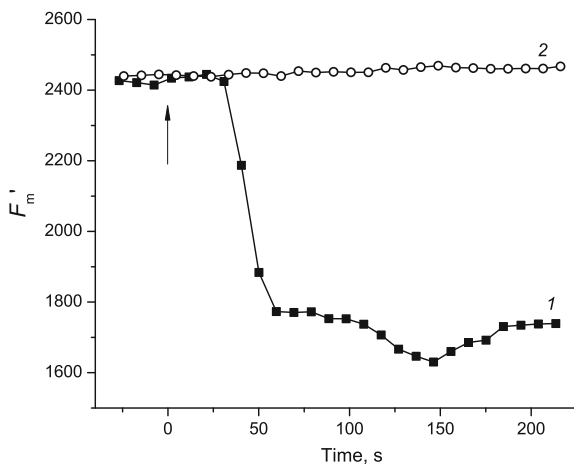streamed away from AOI (curve 2).

Fig. 12.2 Asymmetric changes in chlorophyll fluorescence F_m' on a microscopic area of the chloroplast layer in *C. corallina* cell upon the onset of localized illumination (500 µmol m^{-2} s^{-1}) directed through a 0.4 mm-wide optic fiber adjusted in two different positions: (*1*) 1 mm upstream of analyzed cell region (AOI) with regard to the direction of cytoplasmic flow and (*2*) 1 mm downstream of AOI. The spot light was superimposed on permanent background illumination of the whole cell (28 µmol m^{-2} s^{-1}). The *arrow* marks the moment when localized light was switched on

12.4.2 Inhibition of Photosynthesis by Inflow of "Irradiated Cytoplasm"

The F_m' changes induced by continuous localized light applied upstream of AOI showed complex nonmonotonic kinetics. Short light pulses induced smaller F_m' transients of a simpler shape. These F_m' changes can be expressed after recalculation as changes in NPQ that increases with lowering of F_m'. The plot of NPQ as a function of light pulse duration fits to an S-shaped Boltzmann curve. The initial concave portion of the fitting curve contains information on the period (15–20 s) during which some effector substance is produced inside brightly illuminated chloroplasts and released into the flow. Alternatively, it may reflect the period during which some metabolite essential for photosynthesis is depleted in chloroplasts and starts declining in the cytoplasm.

Comparatively short light pulses applied upstream of AOI (20–45 s) induced the F_m' changes that started and developed after the end of light pulse. The time lapse as long as 100 s between the end of a light pulse and the peak of NPQ could be observed at large separation distances between the light spot and AOI.

The light pulses of 30–60 s duration, applied upstream of AOI, induced F_m' responses with roughly symmetrical front and rear slopes. Such responses, reminiscent of peaks in elution chromatography, can be fitted to Gaussian curves. Figure 12.3 shows the peak position on the F_m'-fitting curves as a function of
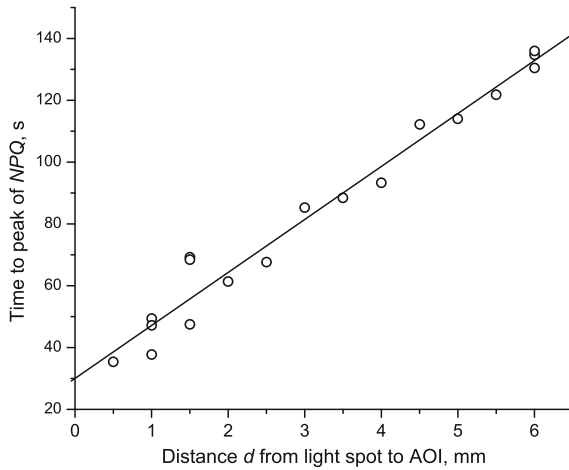
Fig. 12.3 Position of NPQ peak (F_m' minimum) on fitted curves of the pulse-induced quenching response as a function of distance between AOI and 0.4 mm optic fiber located upstream of AOI. The light pulse duration was 30 s, the intensity of permanent background light was 25 µmol m^{-2} s^{-1}. The inverse of the slope for the given internode (≈ 60 µm/s) falls into the range of streaming velocities. The time is given relative to the time point at which the light pulse was switched on

distance d between AOI and the irradiation point. The larger was the distance between the light spot and AOI, the longer time was needed to observe the F_m' dip (NPQ peak). The inverse of the slope of this linear plot (expressed in µm/s) was in the range of velocities typical of cytoplasmic streaming in Characean cells. The velocity of mediator movement was calculated with a simplifying assumption of linear, rather than the helical flow. The actual traveling distance along the helical path of cytoplasmic flow is higher than the separation distance d by the factor defined from the helix pitch distance and the cell diameter. The calculated rate of the mediator movement with the allowance for helical path will be respectively higher.

The ordinate segment corresponding to zero distance d in Fig. 12.3 (30 s) represents the time of the complete stimulus–response cycle except for the step of mediator migration with the streaming cytoplasm. About half of this time is attributed to the release of the messenger from brightly illuminated chloroplasts to the liquid flow or, alternatively, to the depletion of some essential metabolite from the cytoplasm. Another half represents the exchange of the intermediate between streaming cytoplasm and chloroplasts in the shaded area, which is followed by NPQ development.

The amplitude of cyclosis-mediated F_m' change was lowered with increasing distance d between AOI and the light guide position. Nevertheless, at a distance of 6 mm between the light spot and AOI, the cyclosis-mediated F_m' changes constituted about 25% of the response observed at a 1 mm distance.

12.4.3 Stimulation of Photosynthesis by Inflow of "Darkened Cytoplasm"

The drop of F_m' in AOI in Fig. 12.2 implies that the PSII efficiency declines upon the inflow of "irradiated" cytoplasm, because the cytoplasmic composition promotes the dissipation of excess excitation energy to heat. On the other hand, the inflow of cytoplasm from darkened regions to moderately lit cell areas was found to promote the PSII activity. Evidence on this point was obtained by comparing light-response curves of the effective quantum yield of PSII-driven electron flow $\Delta F/F_m'$ when the whole cell or a small cell part were exposed to light of the same quality and intensity under conditions of active cyclosis and after inhibition of streaming with the actin inhibitor, CB (Bulychev and Dodonova 2011).

In the untreated cell the gradual increase of PFD to 100 μmol m^{-2} s^{-1} was accompanied by the sigmoid decrease in $\Delta F/F_m'$ under illumination of entire cell, but had little effect on $\Delta F/F_m'$ when the major cell part was screened while only a 2 mm cell portion with AOI in the center was irradiated. After inhibition of cyclosis with CB, the light-response curve of $\Delta F/F_m'$ assessed under overall illumination remained almost unchanged, whereas the light curve obtained with the narrow light beam was modified and became similar to that observed under whole-cell lighting.

Thus, the light-response curves for PSII quantum yield of electron flow differed substantially under conditions of general and localized illumination but these differences vanished upon the cessation of cyclosis. It means that the interruption of cyclosis-mediated communication between shaded and illuminated cell regions diminishes the photosynthetic activity of locally illuminated chloroplasts at elevated irradiances. It also suggests that the arrival of cytoplasm from darkened cell regions is beneficial for photosynthetic efficiency (increase in $\Delta F/F_m'$), whereas the flow of cytoplasm from irradiated regions reduces $\Delta F/F_m'$. The effect of CB on the light-response curves was reversed upon the recovery of cyclosis after cell washing with a fresh medium.

It should be noted that cyclosis-mediated interactions are only evident when the cell parts communicating through lateral transport are metabolically nonuniform, e.g., exhibit dark and photosynthetic metabolism, as it probably occurs under the imposed light gradient or natural mosaic illumination. Conversely, the lateral transport of uniformly composed cytoplasm along evenly illuminated cells is analogous in many respects to the lack of lateral exchange. It is presently unknown whether the cytoplasm modified by strong light is depleted in some essential component (e.g., inorganic carbon or phosphate) or enriched with some messenger substance or metabolite. The occurrence of chloroplast responses far away (up to 6 mm) from the illumination site and a long delay of their appearance (up to 100 s) after the extinguished flash are relevant to photosynthesis under flickering light commonly encountered by charophytes in natural environments.
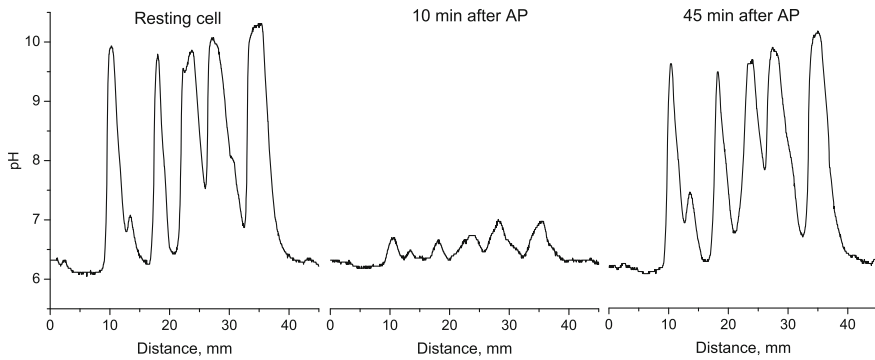
Fig. 12.4 Transient inhibition of light-dependent pH banding in a *C. corallina* cell after the propagation of an electrically triggered action potential (AP). Longitudinal pH profiles near the cell surface were measured (*left*) before AP, (*central*) 10 min after the propagation of a single AP, and (*right*) 45 min after the AP propagation

12.5 Effects of Membrane Excitation on Photosynthetic and pH Patterns

The light–dark transitions are the main factors causing reversible elimination and restoration of pH bands in Characean cells. However, the electrical excitation of cell membranes (action potential, AP) was found to override the influence of continuous light, causing the pH pattern to collapse temporarily despite the ongoing illumination (Bulychev et al. 2004; Krupenina et al. 2008). Although the duration of individual AP is only 3–5 s, the effects of this signal on H^+ transport and photosynthesis persist for 15–30 min.

12.5.1 Transient Collapse of the pH Pattern

The pH_o profile along the internodal cell of *C. corallina* undergoes striking changes upon the electrical excitation of PM with a short pulse of electric current. In the resting cell the pH profile is composed of few alkaline peaks and acidic zones with pH_o shifts as large as 3.5 units (Fig. 12.4). Within about 10 min after the AP generation, the alkaline peaks diminished strongly and the pH profile was largely flattened. The banding profile was restored almost completely within 40 min after the AP generation. Using serial pH profiles, acquired at regular intervals before and after triggering the AP, 3D (time–space) diagrams were plotted to visualize the dynamics of pH patterns after electrical excitation of PM (Krupenina et al. 2008). The decay of pH pattern after AP was similar to that upon darkening but it started with a shorter lag period (Bulychev and Kamzolkina 2006). The decay of pH bands is controlled by diffusion in the unstirred layers

between the acid and alkaline zones and between the unstirred layers and the bulk medium (Bulychev and Krupenina 2010). The recovery of alkaline bands after the AP-induced decline started earlier at higher PFD and elevated concentrations of external Ca^{2+} (Eremin et al. 2007).

The pH_o changes in the acid zone are comparatively small and not resolved in Fig. 12.4. However, when the pH sensor was positioned in the acid zone, it recorded the pH_o increase after AP generation with the amplitude of 0.3–0.35 pH units. Particularly large AP-induced pH changes in the acid zones (up to 0.9 unit) were observed in cells treated with dithiothreitol (DTT) known to reduce disulfide bonds (Dodonova et al. 2010). Based on the notion that the acid cell regions possess H^+-pump activity while the alkaline zones feature high passive conductance for H^+ or OH^-, it was supposed that the AP inhibits temporally both the ATPase-driven H^+ efflux and the passive H^+ influx (OH^- efflux) in different cell regions.

Ionic fluxes during AP in plants comprise the Ca^{2+} influx into the cytoplasm through voltage-gated PM channels, which is followed by the Cl^- efflux through Ca^{2+}-activated channels, and the delayed K^+ efflux (Lunevsky et al. 1983; Beilby 2007). The increase in cytosolic Ca^{2+} content is greatly contributed by the release of Ca^{2+} from intracellular stores (Thiel et al. 2002). The role of AP in osmotic regulation is related to large Cl^- and K^+ effluxes from the cytoplasm to the apoplast during cell excitation. During AP plant cells may lose appreciable quantities of these osmolytes and undergo turgor movements. However, on a relative scale the changes in cytoplasmic Cl^- and K^+ levels during excitation are incomparably smaller than the change in Ca^{2+} level, which increases from the resting level of ~ 0.1 to the order of 10 μM (Williamson and Ashley 1982; Berestovsky and Kataev 2005). High levels of cytosolic Ca^{2+} were reported to inhibit H^+ extrusion by the PM H^+-ATPase (Sehnke et al. 2002), which is in line with the inhibitory effect of AP on acid bands.

12.5.2 Inactivation of High pH Channels

The origin of temporal elimination of alkaline bands after membrane excitation was partly clarified from parallel measurements of AP-induced changes in pH_o, membrane resistance (R_m), and membrane potential (V_m) in electrically insulated alkaline cell areas (Bulychev and Krupenina 2009). The R_m values in these cell regions at rest were low, corresponding to a high membrane conductance (~ 8.3 S/m^2), which falls into the reported range of 5–15 S/m^2 (Smith and Walker 1985). After the AP generation, R_m was found to increase several fold (by a factor of 7.5 in Fig. 12.5a) within about 40 s. The membrane conductance, G_m decreased accordingly. The increase in R_m was paralleled by a large (50–60 mV) hyperpolarization of V_m and by lowering of pH_o. The AP-induced changes in R_m, V_m, and pH_o returned to their initial values within 15 min or longer depending on the irradiance.

Comparison of R_m and pH_o kinetics in alkaline zones after AP (Fig. 12.5b) showed that the peak of R_m was attained much earlier than the minimum of pH_o
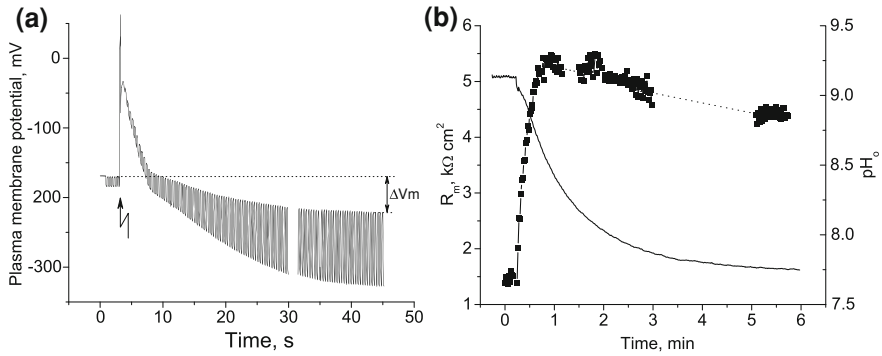
Fig. 12.5 Changes in plasmalemma potential (V_m), resistance (R_m), and surface pH (pH$_o$) in space-clamped alkaline region of *C. corallina* cell upon triggering the AP. The AP was evoked after 20-min rest period in continuous blue light (100 μE m^{-2} s^{-1}). The membrane resistance was tested by passing a train of rectangular hyperpolarizing current pulses (1 μA, 160 ms, 3 Hz). **a** The AP-induced increase in R_m concurrent with the V_m hyperpolarization. The R_m values are proportional to V_m shifts induced by pulses of electric current. The double-headed arrow indicates the post-excitation hyperpolarization. **b** Kinetics of AP-induced R_m changes and pH near the outer cell surface

and that the initial stages of R_m recovery proceeded concurrently with the ongoing pH$_o$ decrease. Hence, the conductance inactivation is not the consequence of pH$_o$ decrease but, most probably, is the cause of H$^+$ flux cessation. The AP-induced drop of pH$_o$, paralleled by a hyperpolarizing shift of V_m and by a profound G_m decrease, suggests that the collapse of pH pattern after AP generation involves the suppression of passive electrogenic H$^+$ (OH$^-$) transport in the alkaline cell areas, which might be considered as a rapid inactivation of the high pH channels. Furthermore, it is becoming clear that the origin of high pH$_o$ in alkaline zones of *Chara* cells cannot be attributed to functioning of H$^+$/HCO$_3^-$ symport or OH$^-$/HCO$_3^-$ antiport, as is often suggested. In the case of electroneutral symport or antiport, the cessation of H$^+$ (OH$^-$) transport and the respective pH$_o$ changes would have occurred without the decrease in G_m.

The AP-induced pH shifts in separate zones differed substantially in untreated and DTT-treated cells, indicating that the pattern of extracellular currents depends on the oxidoreduction state of SH-groups. The AP-sensitive inward H$^+$ fluxes, confined normally to alkaline cell regions, became small after the treatment of cell with DTT, despite the enhanced H$^+$ efflux in the acid regions (Dodonova et al. 2010). This modified pattern of H$^+$ flows would mean that the conductance of alkaline cell regions ceased to be the main load for the electrogenic H$^+$-pump after reduction of disulfide bonds. In this case the pump, which remained active and AP-sensitive, could drive not only the HCO$_3^-$/CO$_2$ conversion but also the accumulation of mineral nutrients, e.g., K$^+$, which enters the cell through ion channels distributed uniformly over PM.

12.5.3 Transient Enhancement of Photosynthetic Pattern

Surprisingly, the elimination of pH pattern after triggering the AP is accompanied by temporal enhancement of spatial heterogeneity of fluorescence and electron flow in chloroplasts (Krupenina et al. 2008). The pattern becomes more contrast because the operating PSII efficiency $\Delta F_m/F_m'$ is hardly influenced by AP in the acidic cell regions, whereas $\Delta F_m/F_m'$ drops in alkaline cell regions where it was already low in the resting state.

The obvious dissimilarity in AP-induced changes of photosynthetic and pH bands provide evidence that the AP affects chloroplast functions and the PM H^+-transport through different pathways initiated by the rise in cytoplasmic Ca^{2+} as a common cause. A possible explanation for the enhancement of photosynthetic pattern is that inhibition of H^+-ATPase in the acidic bands and the concurrent cessation of H^+ influx in the alkaline cell areas after AP produce opposite shifts in the cytosolic pH (pH_c) in different cell regions.

The arrest of continuous H^+ inflow after AP would shift the balance toward higher pH_c in alkaline cell regions, while the arrest of H^+ pump would lower pH_c in the acidic cell regions. According to Muto et al. (1982), the shift of pH from 6.5 to 8.0 in suspensions of intact chloroplasts stimulated the light-induced Ca^{2+} uptake by 80%. Therefore, one may expect that the stromal Ca^{2+} concentration would increase to a larger extent after AP in the alkaline cell regions than in the acidic regions. This may account for the stronger inhibition of CO_2 fixation and ATP consumption in the alkaline cell regions compared to acidic areas (Krupenina et al. 2008). These changes would result in thylakoid energization (ΔpH increase) and energy-dependent quenching, provided some form of ΔpH-generating electron transport (e.g., electron transport to O_2 and monodehydroascorbate) is maintained.

In addition to influence on PSII electron flow, the AP generation was found to affect the photoreactions of PSI. Such influence was evident from the redox transients of chlorophyll P700 reflected by photoinduced absorbance changes $\Delta A_{810-870}$ in resting cells exposed to dim light and in the same cells subjected to excitatory electric stimulus prior to measurement (Bulychev and Krupenina 2010).

12.5.4 Impact of AP on Photosynthesis Through Gated Permeation of Xenobiotics

In the presence of biologically active exogenous compounds, like herbicides, growth regulators, etc., the AP generation may influence the photosynthetic pattern via an alternative mechanism, through changes in compartmentation of added chemicals. Water-soluble charged substances whose permeation is strongly hindered by the PM are especially interesting in this respect. A cationic redox mediator methyl viologen (MV) is an example of xenobiotics generating reactive oxygen species (ROS) (Dodge 1989). The herbicidal action of MV is due to its

efficient reduction by electrons received from PSI, which is followed by reaction with oxygen and ROS production. The oxidized and reduced forms are recycled during MV operation, so that very low catalytic amounts of MV are quite effective.

Chlorophyll fluorescence measurements in *Chara* cells showed that the divalent cation of MV (MV^{2+}) does not pass across the permeability barriers (plasmalemma and chloroplast envelope) in the resting cell, but gains an immediate access to the sites of its interaction with PSI after the AP generation (Bulychev and Krupenina 2008a). Hence, the onset of herbicide action on chloroplasts in vivo coincides with the moment of AP stimulation. This notion was confirmed by the lack of any MV effect on light-induced redox changes of P700 (PSI reaction center chlorophyll and primary electron donor) in the resting cell and by drastic irreversible alteration of P700 photoreduction kinetics after triggering a single AP (Bulychev and Krupenina 2008b)

A better understanding of the AP action in the presence of MV came from analysis of spatiotemporal dynamics of chlorophyll fluorescence (Krupenina et al. 2011). The PM excitation was found to exert different influence on photosynthetic patterns of electron flow and NPQ in the absence and presence of MV in the external medium. Under physiological conditions the AP-induced NPQ and $\Delta F/F_m'$ changes were reversible and manifested mostly in the alkaline regions. By contrast, the quenching evoked by a single AP in the presence of MV was irreversible and was stronger in the acid regions than in the alkaline areas. The spatial heterogeneity of $\Delta F/F_m'$ and NPQ was transiently enhanced after the AP generation in the absence of MV, but the patterns were irreversibly smoothed after evoking an AP in the presence of MV. These findings emphasize different processes underlying the AP-induced NPQ in the absence and in the presence of the redox-cycling agent MV.

The physiological Ca^{2+}-mediated pathway, leading to fluorescence quenching after AP generation (see Sect. 12.5.3), comprises the increase in cytoplasmic Ca^{2+} level, Ca^{2+} entry into the stroma of illuminated chloroplasts, inhibition of the Calvin cycle reactions and ATP consumption, the replacement of CO_2-dependent electron pathway with O_2-dependent electron flow, and the resulting increase in ΔpH as the cause of NPQ increase (Krupenina and Bulychev 2007; Krupenina et al. 2008). Unlike this natural mechanism, the AP-triggered quenching in the presence of MV arises because the AP opens a gate for rapid penetration of the MV into the cell and into the chloroplast stroma where it catalyzes the reduction of O_2 by PSI. The products of this reaction are superoxide anions, converted by superoxide dismutase to H_2O_2. The subsequent enzymatic decomposition of H_2O_2 catalyzed by ascorbate peroxidase produces monodehydroascorbate, which is an effective electron acceptor from PSI (Asada 1999). The increase in NPQ is caused by inhibition of CO_2 fixation and by enhanced ΔpH due to the decrease in ATP demand and stimulation of O_2-dependent electron flow ("water–water cycle"). The critical step in this mechanism is the passage of MV through the membrane pores turned open during the electrical excitation.

The calcium-permeable channel of PM is not strictly selective: the pore diameter of 0.8 nm (Berestovsky, personal communication) is sufficiently large to

pass MV whose ionic radius is 0.33 nm. Therefore Ca^{2+} and MV may compete for the entry into the cytoplasm during the AP. In accord with this notion, the elevated Ca^{2+} concentration (2 mM instead of 0.1 mM) in the external medium prevented the AP-triggered permeation of MV, which was evident from the lack of F_m' quenching. After subsequent lowering of external Ca^{2+} level, the MV-mediated quenching of F_m' appeared immediately after the AP generation. It is possible that the Ca^{2+} binding to PM near the channel at elevated Ca^{2+} level affects the electrostatic field around the pore, thus preventing the permeation of MV^{2+}.

The results demonstrate the potential possibility for the control over MV toxicity in plants and show that permeation of MV through the membrane cell barriers might be promoted by the electric signals propagated over the plants. The electric pulses in plants arise upon injuries, heating, rapid cooling, mechanical agitation, and ionic changes in the environment (Shepherd et al. 2008). Judging from experiments with Characean internodes as a model plant system, it is not excluded that stimulatory impact of AP on the effectiveness of MV treatment can be enhanced or suppressed by adjusting the ionic composition of the external medium.

12.5.5 Effects of Membrane Excitation on Fluorescence Under Localized Lighting

The AP-induced changes in fluorescence and photosynthetic electron transport under uniform illumination occur at a narrow range of light intensities. They are not observed in darkness because linear electron transport coupled with H^+ pumping into the thylakoid is a precondition of their appearance. On the other hand, when the light intensity exceeds a certain threshold, nonphotochemical quenching develops, which diminishes $\Delta F/F_m'$ and F_m' and their sensitivity to AP generation. By contrast, in cells exposed to narrow light beam, $\Delta F/F_m'$ remained high and NPQ remained low even at high light intensities (Sect. 12.4.3), pointing to the possibility that the AP-induced responses may occur at a wider PFD range.

Effects of AP generation on F_m' fluorescence under localized lighting might differ from those under overall illumination because the cytoplasmic flow in the resting cell and the streaming stoppage on the peak of AP become additional factors affecting the chloroplast–PM interactions under spot illumination. When the whole cell is illuminated, the effects of streaming and of its cessation on $\Delta F/F_m'$ and F_m' are not so much evident (Sect. 12.4.3).

Indeed, the F_m' changes caused by the electrical excitation of PM differed substantially depending on the illumination pattern (whole-cell versus partial illumination), even though the wavelengths and irradiance were identical in both cases (Bulychev and Dodonova 2011). In a cell exposed to PFD of 45 and 71 $\mu mol\ m^{-2}\ s^{-1}$, the AP triggered at lower irradiance was followed by the F_m' decrease under whole-cell illumination but was without effect in the case of small area illumination (Fig. 12.6). At elevated PFD, the electrical excitation
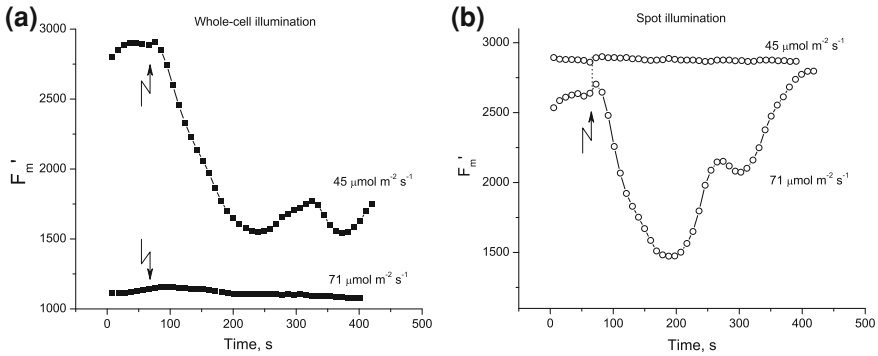
Fig. 12.6 Changes in F_m' chlorophyll fluorescence triggered by generation of the AP (*zigzag arrows*) under **a** whole-cell illumination (*solid symbols*), and **b** illumination of a 2 mm wide cell area (*open circles*) at PFD of 45 and 71 μmol m^{-2} s^{-1}

resulted in F_m' quenching under illumination of a small cell area but had no effect on F_m' under overall illumination, since F_m' was already quenched by light at this PFD.

When an intense narrow beam was applied to AOI through the optic fiber, while the rest part of the cell was kept in darkness, the initial rapid quenching of F_m' was followed by the release of quenching within about 3 min, indicating the activation of CO_2 fixation. A surprising point is that NPQ was low under steady state despite the intense incident light. This was apparently due to continuous inflow of "dark" cytoplasm to AOI. By contrast, when the spot beam was applied in addition to weak illumination of the whole cell, it caused a sustained decrease in F_m', even though the background light was almost 20 times weaker than the spot beam. It means that the composition of cytoplasm arriving from dimly illuminated cell parts differed from that arriving from darkened areas and sufficed to quench fluorescence after the AP propagation.

In the area of intense local illumination, the F_m' response to AP generation was manifested even at a high intensity light directed through the 0.4 mm optic fiber (Bulychev and Dodonova 2011). Thus, a continuous flow of cytoplasm from the darkened to illuminated cell regions not only enhanced the chloroplast photosynthetic activity but also shifted and broadened the range of F_m' responses to membrane excitation.

It appears that NPQ induced by AP in locally illuminated cells originates from two basic causes. One is the onset of the Ca^{2+}-mediated pathway, also operative when the AP is generated under overall illumination. The other is a sudden cessation of cytoplasmic streaming, which arrests the permanent renewal of the cytoplasm around the chloroplasts in the illuminated area. This would immediately affect the substrate and metabolite exchange across the chloroplast envelope, giving rise to NPQ and suppression of electron flow.

Nevertheless, the effect of AP on F_m' and $\Delta F/F_m'$ cannot be entirely assigned to the stoppage of streaming. Such effects of membrane excitation are readily observed under whole-cell illumination, at which the cessation of cytoplasmic streaming had a minor effect on PSII efficiency (Sect. 12.4.3). The basic similarity of electrical signal-induced fluorescence responses in *Chara* and in small-sized cells of plant leaves also argues against such possibility, because influence of streaming on photosynthesis is presumably weaker in mesophyll cells, where cyclosis rates and the light heterogeneity at the cell level are lower than in Characean cells.

The shift of AP-induced F_m' transients toward the elevated PFD range under localized lighting is possibly due to the existence of some laterally transportable cytoplasmic component whose level is modulated by both photosynthetic metabolism and by the electrical excitation of PM. Calcium is one of the candidates for this role because its cytoplasmic level is modulated by light (Johnson et al. 2006; Harada and Shimazaki 2009) and by the electrical excitation of the cell. At variance with earlier reports, the photosynthetically active light was found to induce rapid transient increase in cytosolic Ca^{2+} level (Harada and Shimazaki 2009), which is similar to the cytosolic Ca^{2+} rise upon the electrical membrane excitation in plant cells.

12.6 Conclusion

Internodal cells of *Chara corallina* represent a unique model system to study interactions between photosynthesis, membrane excitation, and cytoplasmic streaming, as well as the role of these processes in generation and regulation of functional patterns in green cells and tissues. It is established that the inflow of cytoplasm from darkened cell parts promotes photosynthetic activity of chloroplasts residing at intermediate irradiance, whereas the delivery of cytoplasm from illuminated regions suppresses this activity and enhances nonphotochemical quenching. The vectorial movement of the "irradiated" cytoplasm induces functional asymmetry (pattern formation) both in the chloroplast layer and in the PM. The signal transferred between illuminated and shaded cell parts was found to move at the velocity of cytoplasmic streaming. The effects of membrane excitation (action potential) on photosynthesis and membrane H^+ transport are area specific; they are also mediated by different mechanisms under physiological conditions and in the presence of some redox-cycling compounds. The influence of action potential on chlorophyll fluorescence under spot illumination appears to involve both the activation of Ca^{2+}-mediated pathways and the stoppage of cyclosis. The cytoplasmic flow from darkened to illuminated cell parts enhances interactions between respiratory and light-dependent metabolism, which promotes photosynthesis and protects chloroplasts from photooxidative damage under excess light.

References

Asada K (1999) The water–water cycle in chloroplasts: scavenging of active oxygen and dissipation of excess photons. Ann Rev Plant Physiol Plant Mol Biol 50:601–639

Baker NR (2008) Chlorophyll fluorescence: a probe of photosynthesis in vivo. Annu Rev Plant Biol 59:89–113

Beilby MJ (2007) Action potential in charophytes. Int Rev Cytol 257:43–82. doi:10.1016/S0074-7696(07)57002-6

Beilby MJ, Mimura T, Shimmen T (1993) The proton pump, high pH channels, and excitation: voltage clamp studies of intact and perfused cells of *Nitellopsis obtusa*. Protoplasma 175:144–152

Berestovsky GN, Kataev AA (2005) Voltage-gated calcium and Ca^{2+}-activated chloride channels and Ca^{2+} transients: voltage-clamp studies of perfused and intact cells of *Chara*. Eur Biophys J 34:973–986. doi:10.1007/s00249-005-0477-9

Bisson MA, Walker NA (1980) The *Chara* plasmalemma at high pH. Electrical measurements show rapid specific passive uniport of H^+ or OH^-. J Membr Biol 56:1–7

Borowitzka MA (1987) Calcification in algae: mechanisms and the role of metabolism. Crit Rev Plant Sci 6:1–45

Bradley MO (1973) Microfilaments and cytoplasmic streaming: inhibition of streaming with cytochalasin. J Cell Sci 12:327–343

Braun M, Foissner I, Lühring H, Schubert H, Thiel G (2007) Characean algae: still a valid model system to examine fundamental principles in plants. Progr Bot 68:193–220

Bulychev AA, Dodonova SO (2011) Effects of cyclosis on chloroplast–cytoplasm interactions revealed with localized lighting in characean cells at rest and after electrical excitation. Biochim Biophys Acta 1807:1221–1230. doi:10.1016/j.bbabio.2011.06.009

Bulychev AA, Kamzolkina NA (2006) Differential effects of plasma membrane electric excitation on H^+ fluxes and photosynthesis in characean cells. Bioelectrochemistry 69:209–215. doi:10.1016/j.bioelechem.2006.03.001

Bulychev AA, Krupenina NA (2008a) Action potential opens access for the charged cofactor to the chloroplasts of *Chara corallina* cells. Russ J Plant Physiol 55:175–184. doi:10.1134/S1021443708020039

Bulychev AA, Krupenina NA (2008b) Facilitated permeation of methyl viologen into chloroplasts in situ during electric pulse generation in excitable plant cell membranes. Biochem (Moscow), Suppl Series A: Membr Cell Biol 2:387–394. doi:10.1134/S1990747808040132

Bulychev AA, Krupenina NA (2008c) Effects of plasma membrane excitation on spatially distributed H^+ fluxes, photosynthetic electron transport and non-photochemical quenching in the plant cell. In: Bernstein EM (ed) Bioelectrochemistry research developments. Nova Science Publishers, New York

Bulychev AA, Krupenina NA (2009) Transient removal of alkaline zones after excitation of *Chara* cells is associated with inactivation of high conductance in the plasmalemma. Plant Signal Behav 4:727–734

Bulychev AA, Krupenina NA (2010) Physiological implications of action potential in characean cell: effects on pH bands and spatial pattern of photosynthesis. In: DuBois ML (ed) Action potential: biophysical and cellular context, initiation, phases and propagation. Nova Science Publishers, New York

Bulychev AA, Vredenberg WJ (2003) Spatio-temporal patterns of photosystem II activity and plasma-membrane proton flows in *Chara corallina* cells exposed to overall and local illumination. Planta 218:143–151. doi:10.1007/s00425-003-1084-6

Bulychev AA, Cherkashin AA, Rubin AB, Vredenberg WJ, Zykov VS, Müller SC (2001a) Comparative study on photosynthetic activity of chloroplasts in acid and alkaline zones of *Chara corallina*. Bioelectrochemistry 53:225–232

Bulychev AA, Polezhaev AA, Zykov SV, Pljusnina TY, Riznichenko GY, Rubin AB, Jantoss W, Zykov VS, Müller SC (2001b) Light-triggered pH banding profile in *Chara* cells revealed with a scanning pH microprobe and its relation to self-organization phenomena. J Theor Biol 212:275–294. doi:10.1006/jtbi.2001.2375

Bulychev AA, Zykov SV, Rubin AB, Müller SC (2003) Transitions from alkaline spots to regular bands during pH pattern formation at the plasmalemma of *Chara* cells. Eur Biophys J 32: 144–153. doi:10.1007/s00249-003-0280-4

Bulychev AA, Kamzolkina NA, Luengviriya J, Rubin AB, Müller SC (2004) Effect of a single excitation stimulus on photosynthetic activity and light-dependent pH banding in *Chara* cells. J Membr Biol 202:11–19. doi:10.1007/s00232-004-0716-5

Bulychev AA, Van den Wijngaard PWJ, De Boer AH (2005) Spatial coordination of chloroplast and plasma membrane activities in *Chara* cells and its disruption through inactivation of 14-3-3 proteins. Biochemistry (Moscow) 70:55–61

Coelho SMB, Brownlee C, Bothwell JHF (2008) A tip-high, Ca^{2+}-interdependent, reactive oxygen species gradient is associated with polarized growth in *Fucus serratus* zygotes. Planta 227:1037–1046. doi:10.1007/s00425-007-0678-9

Davies E (2006) Electrical signals in plants: facts and hypotheses. In: Volkov A (ed) Plant electrophysiology theory and methods. Springer, Berlin

Dodge A (1989) Herbicides interacting with photosystem I. In: Dodge A (ed) Herbicides and plant metabolism. Cambridge University Press, Cambridge

Dodonova SO, Bulychev AA (2011) Cyclosis-related asymmetry of chloroplast–plasma membrane interactions at the margins of illuminated area in *Chara corallina* cells. Protoplasma 248(4):737–749. doi:10.1007/s00709-010-0241-6

Dodonova SO, Krupenina NA, Bulychev AA (2010) Suppression of the plasma membrane H^+-conductance on the background of high H^+-pump activity in dithiothreitol-treated *Chara* cells. Biochem (Moscow), Suppl Series A Membr Cell Biol 4:389–396. doi:10.1134/S1990747810040094

Dorn A, Weisenseel MH (1984) Growth and the current pattern around internodal cells of *Nitella flexilis* L. J Exp Bot 35:373–383

Eremin A, Bulychev A, Krupenina NA, Mair T, Hauser MJB, Stannarius R, Müller S, Rubin AB (2007) Excitation-induced dynamics of external pH pattern in *Chara corallina* cells and its dependence on external calcium concentration. Photochem Photobiol Sci 6:103–109. doi:10.1039/b607602e

Feijo JA, Sainhas J, Hackett GR, Kunkel JG, Hepler PK (1999) Growing pollen tubes possess a constitutive alkaline band in the clear zone and a growth-dependent acidic tip. J Cell Biol 144:483–496

Felle HH (1998) The apoplastic pH of the *Zea mays* root cortex as measured with pH-sensitive microelectrodes: aspects of regulation. J Exp Bot 49:987–995

Finazzi G, Johnson GN, Dallosto L, Joliot P, Wollman F-A, Bassi R (2004) A zeaxanthin-independent nonphotochemical quenching mechanism localized in the photosystem II core complex. Proc Natl Acad Sci U S A 101:12375–12380. doi:10.1073/pnas.0404798101

Foissner I (2004) Microfilaments and microtubules control the shape, motility, and subcellular distribution of cortical mitochondria in characean internodal cells. Protoplasma 224:145–157. doi:10.1007/s00709-004-0075-1

Foissner I, Wasteneys GO (2007) Wide-ranging effects of eight cytochalasins and latrunculin A and B on intracellular motility and actin filament reorganization in characean internodal cells. Plant Cell Physiol 48:585–597. doi:10.1093/pcp/pcm030

Fromm J (2006) Long-distance electrical signaling and physiological functions in higher plants. In: Volkov A (ed) Plant electrophysiology theory and methods. Springer, Berlin

Fromm J, Lautner S (2007) Electrical signals and their physiological significance in plants. Plant, Cell Environ 30:249–257. doi:10.1111/j.1365-3040.2006.01614.x

Goldstein RE, Tuval I, Van de Meent J-W (2008) Microfluidics of cytoplasmic streaming and its implications for intracellular transport. Proc Natl Acad Sci U S A 105:3663–3667. doi:10.1073/pnas.0707223105

Gow NAR, Kropf DL, Harold FM (1984) Growing hyphae of *Achlya bisexualis* generate a longtitudinal pH gradient in the surrounding medium. J Gen Microbiol 130:2967–2974

Grams TEE, Lautner S, Felle HH, Matyssek R, Fromm J (2009) Heat-induced electrical signals affect cytoplasmic and apoplastic pH as well as photosynthesis during propagation through the maize leaf. Plant, Cell Environ 32:319–326. doi:10.1111/j.1365-3040.2008.01922.x

Hager A (2003) Role of the plasma membrane H^+-ATPase in auxin-induced elongation growth: historical and new aspects. J Plant Res 116:483–505. doi:10.1007/s10265-003-0110-x

Hansen U-P, Moldaenke C, Tabrizi H, Ramm D (1993) The effect of transthylakoid proton uptake on cytosolic pH and the imbalance of ATP and $NADPH/H^+$ production as measured by CO_2- and light-induced depolarization of the plasmalemma. Plant Cell Physiol 34:681–695

Harada A, Shimazaki K (2009) Measurement of changes in cytosolic Ca^{2+} in *Arabidopsis* guard cells and mesophyll cells in response to blue light. Plant Cell Physiol 50:360–373. doi:10.1093/pcp/pcn203

Jansson C, Northen T (2010) Calcifying cyanobacteria—the potential of biomineralization for carbon capture and storage. Curr Opin Biotechnol 21:1–7. doi:10.1016/j.copbio.2010.03.017

Johnson CH, Shingles R, Ettinger WF (2006) Regulation and role of calcium fluxes in the chloroplast. In: Wise RR, Hoober JK (eds) The structure and function of plastids. Springer, Dordrecht

Kamiya N (1959) Protoplasmic streaming. Springer, Wien

Koziolek C, Grams TEE, Schreiber U, Matyssek R, Fromm J (2003) Transient knockout of photosynthesis mediated by electrical signals. New Phytol 161:715–722. doi:10.1046/j.1469-8137.2003.00985.x

Krol E, Dziubinska H, Trebacz K (2010) What do plants need action potentials for? In: DuBois ML (ed) Action potential: biophysical and cellular context, initiation, phases and propagation. Nova Science Publisher, New York

Krupenina NA, Bulychev AA (2007) Action potential in a plant cell lowers the light requirement for non-photochemical energy-dependent quenching of chlorophyll fluorescence. Biochim Biophys Acta 1767:781–788. doi:10.1016/j.bbabio.2007.01.004

Krupenina NA, Bulychev AA, Roelfsema MRG, Schreiber U (2008) Action potential in *Chara* cells intensifies spatial patterns of photosynthetic electron flow and non-photochemical quenching in parallel with inhibition of pH banding. Photochem Photobiol Sci 7:681–688. doi:10.1039/b802243g

Krupenina NA, Bulychev AA, Schreiber U (2011) Chlorophyll fluorescence images demonstrate variable pathways in the effects of plasma membrane excitation on electron flow in chloroplasts of *Chara* cells. Protoplasma 248:513–522. doi:10.1007/s00709-010-0198-5

Lucas WJ (1975a) The influence of light intensity on the activation and operation of the hydroxyl efflux system of *Chara corallina*. J Exp Bot 26:347–360

Lucas WJ (1975b) Photosynthetic fixation of ^{14}carbon by internodal cells of *Chara corallina*. J Exp Bot 26:331–346

Lucas WJ, Dainty J (1977) Spatial distribution of functional OH^- carriers along a characean internodal cell: determined by the effect of cytochalasin B on $H^{14}CO_3^-$ assimilation. J Membr Biol 32:75–92

Lucas WJ, Nuccitelli R (1980) HCO_3^- and OH^- transport across the plasmalemma of *Chara*: spatial resolution obtained using extracellular vibrating probe. Planta 150:120–131

Lunevsky VS, Zherelova OM, Vostrikov IY, Berestovsky GN (1983) Excitation of characeae cell membranes as a result of activation of calcium and chloride channels. J Membr Biol 72:43–58

Marten I, Deeken R, Hedrich R, Roelfsema MRG (2010) Light-induced modification of plant plasma membrane ion transport. Plant Biol 12:64–79. doi:10.1111/j.1438-8677.2010.00384.x

McConnaughey T (1991) Calcification in *Chara corallina*: CO_2 hydroxylation generates protons for bicarbonate assimilation. Limnol Oceanogr 36:619–628

Metraux JP, Richmond PA, Taiz L (1980) Control of cell elongation in *Nitella* by endogeneous cell wall pH gradients. Multiaxial extensibility and growth studies. Plant Physiol 65:204–210

Muto S, Izawa S, Miyachi S (1982) Light-induced Ca^{2+} uptake by intact chloroplasts. FEBS Lett 139:250–254

Nobel PS (2005) Physicochemical and environmental plant physiology. Academic, London

Ogata K, Toko K, Fujiyoshi T, Yamafuji K (1987) Electric inhomogeneity in membrane of characean internode influenced by light-dark transition, O_2, N_2, CO_2-free air and extracellular pH. Biophys Chem 26:71–81

Palmgren MG (1998) Protein gradients and plant growth: role of the plasma membrane H^+-ATPase. Adv Bot Res 28:1–70

Pavlovic A, Slovakova L, Pandolfi C, Mancuso S (2011) On the mechanism underlying photosynthetic limitation upon trigger hair irritation in the carnivorous plant Venus flytrap (*Dionaea muscipula* Ellis). J Exp Bot 62:1991–2000. doi:10.1093/jxb/erq404

Pickard WF (2003) The role of cytoplasmic streaming in symplastic transport. Plant, Cell Environ 26:1–15

Plieth C, Tabrizi H, Hansen U-P (1994) Relationship between banding and photosynthetic activity in *Chara corallina* as studied by the spatially different induction curves of chlorophyll fluorescence observed by an image analysis system. Physiol Plant 91:205–211

Plyusnina TY, Lavrova AI, Riznichenko GY, Rubin AB (2005) Modeling the pH and the transmembrane potential banding along the cell membrane of alga *Chara corallina*. Biophysics 50:434–440

Prins HBA, Snel JFH, Zanstra PE, Helder RJ (1982) The mechanism of bicarbonate assimilation by the polar leaves of *Potamogeton* and *Elodea*. CO_2 concentrations at the leaf surface. Plant, Cell Environ 5:207–214

Rayle DL, Cleland DL (1992) The acid growth theory of auxin-induced cell elongation is alive and well. Plant Physiol 99:1271–1274

Schmölzer PM, Höftberger M, Foissner I (2011) Plasma membrane domains participate in pH banding of *Chara* internodal cells. Plant Cell Physiol 52:1274–1288. doi:10.1093/pcp/pcr074

Schreiber U (2004) Pulse-amplitude (PAM) fluorometry and saturation pulse method. In: Papageorgiou G, Govindjee (eds) Chlorophyll a fluorescence: a signature of photosynthesis. Kluwer Academic Publishers, Dordrecht

Schurr U, Walter A, Rascher U (2006) Functional dynamics of plant growth and photosynthesis—from steady-state to dynamics—from homogeneity to heterogeneity. Plant, Cell Environ 29:340–352. doi:10.1111/j.1365-3040.2005.01490.x

Sehnke PC, DeLille JM, Ferl RJ (2002) Consummating signal transduction: the role of 14-3-3 proteins in the completion of signal-induced transitions in protein activity. Plant Cell 14:S339–S354. doi:10.1105/tpc.010430

Shepherd VA, Beilby MJ, Khazaaly SAS, Shimmen T (2008) Mechano-perception in *Chara* cells: the influence of salinity and calcium on touch-activated receptor potentials, action potentials and ion transport. Plant, Cell Environ 31:1575–1591

Shimmen T, Wakabayashi A (2008) Involvement of membrane potential in alkaline band formation by internodal cells of *Chara corallina*. Plant Cell Physiol 49:1614–1620. doi:10.1093/pcp/pcn136

Shimmen T, Yamamoto A (2002) Induction of a new alkaline band at a target position in internodal cells of *Chara corallina*. Plant Cell Physiol 43:980–983

Shimmen T, Yokota E (2004) Cytoplasmic streaming in plants. Curr Opin Cell Biol 16:68–72. doi:10.1016/j.ceb.2003.11.009

Siebke K, Weis E (1995) Assimilation images of leaves of *Glechoma hederacea*: analysis of non-synchronous stomata related oscillations. Planta 196:155–165

Smith JR, Walker NA (1985) Effects of pH and light on the membrane conductance measured in the acid and basic zones of *Chara*. J Membr Biol 83:193–205

Spear DG, Barr JK, Barr CE (1969) Localization of hydrogen ion and chloride ion fluxes in *Nitella*. J Gen Physiol 54:397–414

Stahlberg R, Cosgrove DJ (1997) The propagation of slow wave potentials in pea epicotyls. Plant Physiol 113:209–217

Takakura T, Fang W (2002) Climate under cover. Kluwer, Dordrecht

Tazawa M (2003) Cell physiological aspects of the plasma membrane electrogenic H^+ pump. J Plant Res 116:419–442. doi:10.1007/s10265-003-0109-3

Thiel G, Wacke M, Foissner I (2002) Ca^{2+} mobilization from internal stores in electrical membrane excitation in *Chara*. Progr Bot 64:217–233

Van Sambeek JW, Pickard BG (1976) Mediation of rapid electrical, metabolic, transpirational, and photosynthetic changes by factors released from wounds. III. Measurements of CO_2 and H_2O flux. Can J Bot 54:2662–2671

Verchot-Lubicz J, Goldstein RE (2010) Cytoplasmic streaming enables the distribution of molecules and vesicles in large plant cells. Protoplasma 240:99–107. doi:10.1007/s00709-009-0088-x

Walker NA, Smith FA, Cathers IR (1980) Bicarbonate assimilation by fresh-water charophytes and higher plants. I. Membrane transport of bicarbonate ions is not proven. J Membr Biol 57:51–58

Williamson RE, Ashley CC (1982) Free Ca^{2+} and cytoplasmic streaming in the alga *Chara*. Nature 296:647–650